

CONF-930511--526

A METHOD FOR MEASURING DARK CURRENT ELECTRON BEAMS IN AN RF LINAC*

X.K. Maruyama, T. Fasanello, H. Rietydy
 Naval Postgraduate School, Monterey, CA 93943

M.A. Piestrup

Adelphi Technology, Palo Alto, CA 94301

D.W. Rule, R.B. Fiorito

Naval Surface Warfare Center, Silver Spring, MD 20903

Abstract

X-ray fluorescence from thin foils inserted into the NPS linac has been used to measure the integrated electron beam intensity when the accelerator is operating with dark current. The measured x-ray flux, the known inner shell ionization cross sections and radiative transition probabilities are used to obtain measurements of dark currents of the order of 10^{-14} Amperes. The same arrangement allows continuous, in-situ energy calibration of our SiLi detector in the electromagnetic noise environment of the linac. This technique was originally developed to perform absolute production efficiency measurements of parametric x-ray generation in the 5 - 50 keV range.

I. INTRODUCTION

The count rate for X-ray spectroscopy experiments are limited by detector characteristics and for large cross section events, the incident electron current must be considerably reduced. In our experiment to measure the characteristics of parametric x-radiation (Bragg scattering of virtual photons)¹, the electron beam from a pulsed s-band linac was restricted to dark current wherein the electron gun was turned off and average currents of the order of 10^{-14} amperes were incident on target (10^{-14} A is approximately 1000 electrons per each 1 μ s macrobunch in our linac). Such small currents presented a challenge in determining the normalization for the absolute production efficiency of x-rays.

A second consideration is the energy calibration of the x-ray spectrum in the linac environment. The detector is energy calibrated against known sources in a static environment. However, x-rays are generated by electrons from a pulsed s-band rf linac wherein they are accelerated in 1 μ s macrobunches. For our

application, the microbunch structure is not a consideration since the detector resolving time is longer than the linac macrobunch time. During the interaction time of the electron with the target, there are sources of noise associated with the linac pulse structure which distort the energy calibration. These include klystron rf noise picked up by the detector preamplifier and ground loop currents. Physical corrections such as rf shielding and grounding of the detector system are only partially successful.

II. X-RAY FLUORESCENCE MEASUREMENTS

Both x-ray energy and electron fluence questions have been successfully addressed by the observation of K fluorescence photons from electron-excited atoms. K energies are well known. Since the electro-excited atomic lifetimes are much shorter than 1 μ s they may be considered to be created within the linac bunch duration. With the knowledge of electron interaction cross sections² and from radiative transition probabilities³, the fluorescent x-ray intensities may be unfolded to obtain the incident electron integrated current. Figure 1 presents a spectrum of fluorescence x-rays obtained from a foil target consisting of a sandwich of titanium, yttrium and tin. For this measurement, the target foil was rotated 30° from normal to the electron beam. 85 MeV electrons were made incident upon the foil targets and x-rays were measured with a Si(Li) detector placed at 45° with respect to the incident electron beam direction. We have also made measurements using other materials such as copper and indium to address other energy calibration markers. By identifying known emission line energies with observed peaks the measured spectrum could be calibrated.

The fluorescence was assumed to be isotropic. Care was made to order the target foils so that the x-rays were generated sequentially in tin, yttrium and titanium in order to insure that the softer x-rays suffered less attenuation. The targets were placed in a vacuum chamber and had to traverse a 25 μ m kapton window, a 1.3 cm air gap and a 50 μ m beryllium window before entering a 5 mm thick Si(Li) detector. Corrections for

* This work was partially supported by the Defense Nuclear Agency, the Naval Postgraduate School and USDOE SBIR Contract (No. DE-FG03-91ER81099).

FG03-91ER81099

1

DISTRIBUTION OF THIS DOCUMENT IS UNLIMITED

MASTER

DISCLAIMER

**Portions of this document may be illegible
in electronic image products. Images are
produced from the best available original
document.**

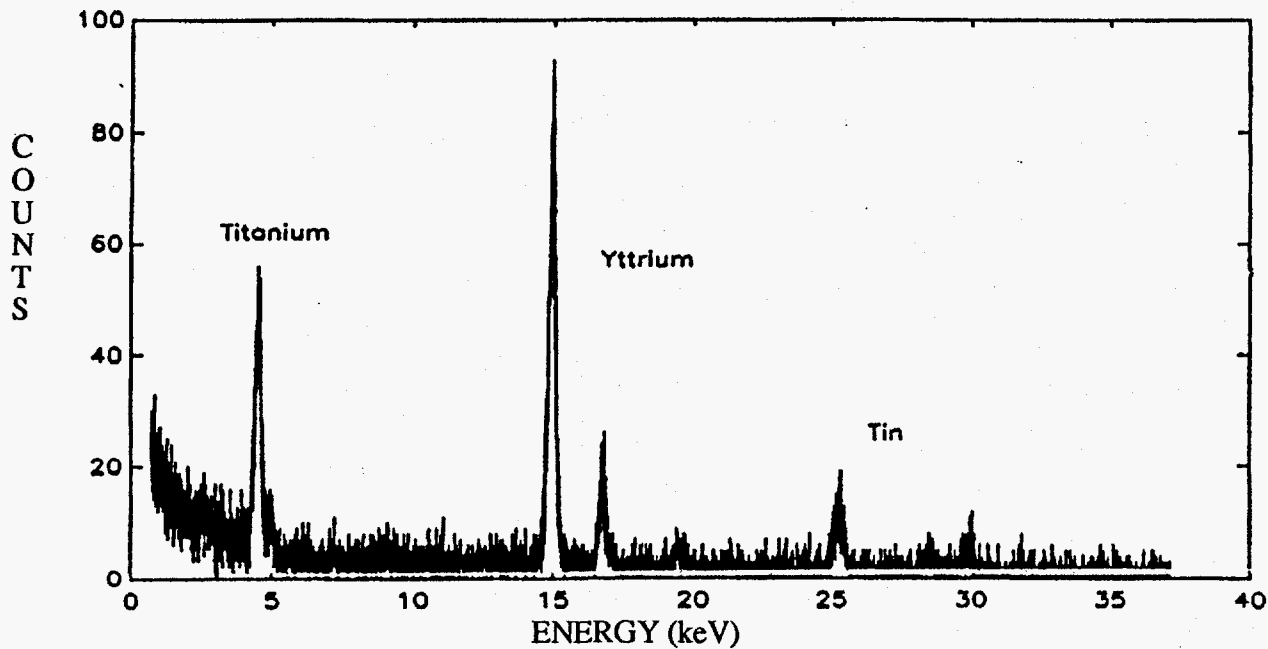


Figure 1. Pulse Height Analysis Spectrum of fluorescent x-rays from a sandwich foil of titanium, yttrium and tin. In Y and Sn the K_{α} and K_{β} lines are observed. Electron beam energy was 85 MeV.

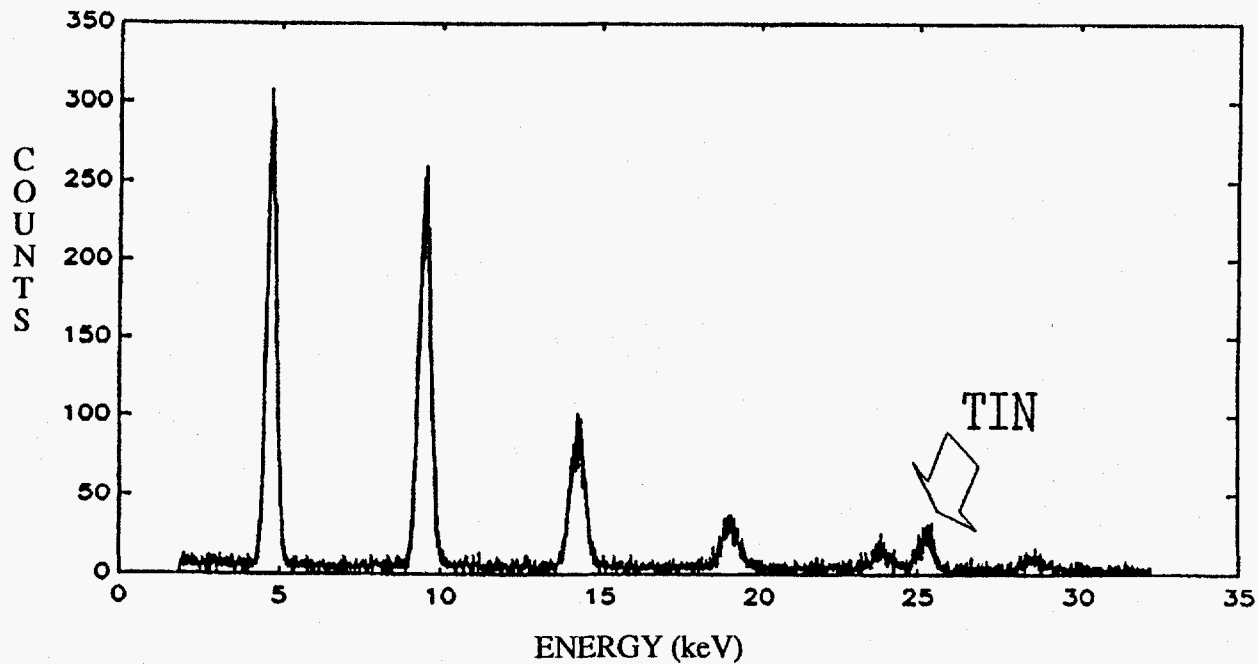


Figure 2. Observed spectrum of parametric x-radiation from a mosaic graphite target. A thin foil of tin behind the PXR target was used to create the calibration peak at 25.2 keV.

attenuation⁴ in the intervening materials were made.

$$N_e = \frac{N_{ph} AW}{\sigma \left(\frac{\Omega_d}{4\pi} \right) \rho N_o f_{det} t_{eff} a \epsilon}$$

where,

N_e = total number of electrons incident on target

N_{ph} = Number of photons detected

AW = Atomic Weight of target (g/mole)

σ = electron interaction cross section (cm²)

Ω_d = detector solid angle

ρ = density of target material (gm/cm²)

N_o = Avogadro's number

f_{det} = radiative transition probability

t_{eff} = effective target thickness (cm)

a = total photon attenuation factor

ϵ = detector efficiency

When two photons arrive within the resolving time of the detector, they are counted as a single photon with energy equal to the sum of the two photons. The inferred average currents when the ratio between linac machine pulses and events counted in the pulse height analyzer was 2:1 differ by over 30 %. When the ratio of machine pulses to observed counts is increased to 7:1, the range of inferred currents is reduced to a more consistent 13 %. The uncertainties presented in these tables mainly reflect the estimated uncertainties of 30 % for the electron-interaction cross section² and 10 % for the radiative transition probabilities³. These uncertainties reflect systematic errors for determination of the absolute integrated beam current.

III. APPLICATION

The method prescribed here was used to both energy calibrate and normalize the spectrum of x-rays from parametric x-radiation¹. Figure 2 presents an observed PXR spectrum. In this observation, a thin foil of tin was placed on the back of a mosaic graphite target from which the PXR peaks of interest were generated. The fluorescent x-rays and the parametric x-rays were measured under identical conditions. PXR peaks are located at integer multiples of the fundamental. By carefully selecting x-ray fluorescence calibration materials, the calibration peak may be made to not interfere with the measurement of the PXR peak. The tin x-ray peaks serves both as an energy marker and as an integrated beam current monitor.

IV. CONCLUSION

By measuring fluorescent x-rays simultaneously with photons generated from parametric x-radiation, an on-line energy and intensity calibration has been determined. This technique can be further exploited for special circumstances. With a soft x-ray detector contained in the same vacuum system as the electron beam, it would be possible to use the x-ray fluorescence from the parametric x-ray generation target. For example, with a crystalline silicon target, 1.8 keV x-rays would have to be detected. For heavier crystals such as silver, the present arrangement would suffice result in K_α x-rays of 22.16 and 21.99 keV and K_β x-rays of 24.9 KeV.

The method described in this paper need not be confined to the measurement of parametric x-radiation, but can be extended to other sources such as channeling⁵ and transition radiation⁶.

	Tin	Yttrium	Titanium
N_{ph}	453±95	2553±194	1214±177
$N_e (10^8)$	9.67±3.67	9.48±3.13	8.57±2.99
$I(10^{-14} A)$	3.70±1.41	3.62±1.19	3.28±1.15

Table I. Number of observed photons, incident electrons and average current. Elapsed time was 4212 s.

V. REFERENCES

1. D.W. Rule, R.B. Fiorito, M.A. Piestrup, C.K. Gary and X.K. Maruyama, "Production of X-rays by the Interaction of Charged Particle Beams with Periodic Structures and Crystalline Materials", SPIE, 1552, p. 240 (1991). See also X.K. Maruyama et al., these Proceedings.
2. S.T. Perkins, D.E. Cullen and S.M. Seltzer, "Tables and Graphs of Electron-Interaction Cross Sections from 10 eV to 100 GeV", LLNL, UCRL-50400 Vol 31 (1991).
3. S.T. Perkins et al., "Tables and Graphs of Atomic Subshell and Relaxation Data Derived from the LLNL Evaluated Atomic Data Library (EADL), Z=1-100", LLNL, UCRL-50400 Vol 30 (1991).
4. J.H. Hubbell, "XCOM: Photon Cross Sections On a Computer", U.S. Department of Commerce, NBSIR 87-3597 (1991).
5. e.g., H. Uberall, B.J. Faraday, X.K. Maruyama and B.L. Berman, "Short-Wavelength Radiation Sources", 1552, p. 198 (1991).
6. e.g., C.I. Pincus et al., "Measurements of X-Ray Emission from Photoabsorption-edge transition radiation", J. Appl. Phys. 72,4300 (1992).

DISCLAIMER

This report was prepared as an account of work sponsored by an agency of the United States Government. Neither the United States Government nor any agency thereof, nor any of their employees, makes any warranty, express or implied, or assumes any legal liability or responsibility for the accuracy, completeness, or usefulness of any information, apparatus, product, or process disclosed, or represents that its use would not infringe privately owned rights. Reference herein to any specific commercial product, process, or service by trade name, trademark, manufacturer, or otherwise does not necessarily constitute or imply its endorsement, recommendation, or favoring by the United States Government or any agency thereof. The views and opinions of authors expressed herein do not necessarily state or reflect those of the United States Government or any agency thereof.
